

1 **Toxicity of differently sized and coated silver nanoparticles to the**  
2 **bacterium *Pseudomonas putida*: risks for the aquatic environment?**

3

4 Marianne Matzke<sup>1\*</sup>, Kerstin Jurkschat<sup>2</sup> & Thomas Backhaus<sup>1</sup>

5 <sup>1</sup>University of Gothenburg, Department of Biological and Environmental Sciences,  
6 Carl Skottsbergs Gata 22 B, 40530 Göteborg/Sweden

7 <sup>2</sup>Department of Materials, Oxford University Begbroke Science Park, Begbroke Hill,  
8 Yarnton, Oxford OX5 1PF, United Kingdom

9 \*Present address corresponding author: Centre for Ecology and Hydrology, Natural Environment  
10 Research Council, Hails Section, Maclean Building, Benson Lane, Crowmarsh Gifford Wallingford,  
11 OX10 8BB, United Kingdom, [martzk@ceh.ac.uk](mailto:martzk@ceh.ac.uk)

12

13 **Abstract**

14 Aim of this study was to describe the toxicity of a set of different commercially  
15 available silver nanoparticles (AgNPs) to the gram-negative bacterium *Pseudomonas*  
16 *putida* (growth inhibition assay, ISO 10712) in order to contribute to their  
17 environmental hazard and risk assessment. Different AgNP sizes and coatings were  
18 selected in order to analyze whether those characteristics are determinants of  
19 nanoparticle toxicity. Silver nitrate was tested for comparison. In general  
20 *Pseudomonas putida* reacted very sensitive towards the exposure to silver, with an  
21 EC<sub>05</sub> value of 0.043 µg L<sup>-1</sup> for AgNO<sub>3</sub> and between 0.13 and 3.41 µg L<sup>-1</sup> for the  
22 different AgNPs (EC<sub>50</sub> values 0.16 µg L<sup>-1</sup> for AgNO<sub>3</sub>, resp. between 0.25 and 13.5  
23 µg L<sup>-1</sup> for AgNPs). As the ionic form of silver is clearly the most toxic, an  
24 environmental hazard assessment for microorganisms based on total silver  
25 concentration and the assumption that AgNPs dissolve is sufficiently protective.

Neither specific coatings nor certain sizes could be linked to increasing or decreasing toxicity. The characterization of particle behavior as well as the total and dissolved silver content in the medium during the exposures was not possible due to the high sensitivity of *Pseudomonas* (test concentrations were below detection limits), indicating the need for further development in the analytical domain. Monitored silver concentrations in the aquatic environment span six orders of magnitude (0.1 – 120000 ng L<sup>-1</sup>), which falls into the span of observed EC<sub>05</sub> values and might hence indicate a risk to environmental bacteria.

## Introduction

Metal and metal oxide Nanoparticles (NPs) are currently the nanoparticles with the highest production volume with an estimated annual use of 320 tons nanosilver (Nowack, Krug and Height 2011). According to the Woodrow Wilson Inventory (<http://www.nanotechproject.org>, November 2013) silver nanoparticles (AgNPs) are the dominating nanomaterial in consumer products. In order to assess whether a significant environmental exposure might result from the continuously increasing use of AgNPs several studies modeled predicted environmental silver concentrations, based on production volumes, the AgNP content in typical consumer products, clearance rates in sewage treatment plants (STPs) and average water flows.

The resulting predicted environmental concentrations of AgNPs in surface waters were in the range between 0.01 and 80 ng L<sup>-1</sup> nano-silver (Mueller and Nowak 2008). Effluents from STPs are expected to contain higher concentrations in the range of 38-127 ng L<sup>-1</sup> nano-silver, (Gottschalk et al. 2010; Gottschalk et al. 2009). Also the steady release of silver via abrasion, wash water and sewage treatment plants bears the risk of a significant accumulation of silver in aquatic and terrestrial ecosystems

51 (Nowak 2010). A recent study from Mitrano and co-workers (2012) found that the  
 52 effluents of a sewage treatment plant in Boulder, Colorado (USA) contained  
 53 concentrations of 100 ng L<sup>-1</sup> AgNPs (determined by single particle ICP-MS) in the  
 54 presence of 60 ngL<sup>-1</sup> dissolved silver.  
 55 The driving factor for using AgNPs in a broad range of health care and consumer  
 56 products such as bandages, surface coatings, medical equipment, food packaging,  
 57 functional clothes and cosmetics is their broad-spectrum antimicrobial properties  
 58 (D'Britto et al. 2011; Marambio-Jones and Van Hoek 2010). However, the beneficial  
 59 antimicrobial effects of silver nanomaterials might become problematic when silver is  
 60 released into the environment as its bactericidal effects might have negative  
 61 consequences for ecosystem health impairing critical bacteria-driven nutrient cycles  
 62 (e.g. nitrogen, phosphorus or sulfur cycling) and more general the biodegradation of  
 63 organic matter.  
 64 Bacteria are usually amongst the most sensitive species, although - depending on the  
 65 tested bacterial species, biotest system and specific particle type resp. ionic silver-  
 66 toxicity values range from ng L<sup>-1</sup> to mg L<sup>-1</sup> silver (e.g. Fabrega et al. 2011;  
 67 Marambio-Jones and Van Hoek 2010).  
 68 The antimicrobial activity of silver can be mainly attributed to interactions of silver  
 69 ions with thiol groups of cellular proteins, leading to their inactivation. Processes such  
 70 as cell respiration, ion transport across membranes, (Marambio-Jones and Van Hoek  
 71 2010), the ATP production and the ability of the DNA to replicate (Feng et al. 2000)  
 72 are affected as a consequence. However, the mechanisms of toxic action for AgNPs  
 73 are still not very well defined (Fabrega et al. 2011). In particular it is still not clear  
 74 whether the effects of AgNPs are dominated by released silver ions or are caused by  
 75 the unique properties of the particles themselves. Literature provides evidence for

76 both particle dominated (Sheng and Yang 2011; Morones et al. 2005) as well as silver  
77 ion dominated toxicity (Navarro et al. 2008). In summary, the following three  
78 mechanisms are currently suggested in the literature to be mainly responsible for the  
79 antimicrobial activity of silver and AgNPs:

80 i) The release of silver ions from silver nanoparticles and the resulting uptake of  
81 these ions into the cells, leading to similar toxicological consequences as an  
82 exposure to silver salts, in particular the generation of reactive oxygen species  
83 (ROS). ROS are in general produced by metals in the presence of dissolved  
84 oxygen and cause DNA damage, uncontrolled oxidation of proteins,  
85 breakdown of membrane functions, and as a result damage to cellular  
86 structures such as mitochondria.

87 ii) Direct interactions of the AgNPs with the membrane lipids leading either to  
88 membrane damage and/or inducing the uptake of the particles into the cells,  
89 where they function as deposits for the release of silver ions. This was  
90 demonstrated especially for the effects of small AgNPs (1-10 nm) on gram-  
91 negative bacteria (e.g. *Escherichia coli*, *Vibrio cholera*, *Pseudomonas*.  
92 *aeruginosa*, Morones et al. 2005).

93 iii) Interaction of AgNPs with sulfur containing membrane proteins of the  
94 membrane cells which will lead to a disruption of the membrane structure.

95 The diversity of bacterial physiology and morphology is a substantial challenge for  
96 investigating the mode of action of AgNPs. Evidence from literature indicates that  
97 gram-negative bacteria are in general more sensitive to the effects of silver and  
98 AgNPs than gram-positive bacteria (Fabrega et al. 2011), which might be due to the  
99 thinner peptidoglycan layer found in the cell wall of gram-negative species.

100 For these reasons *Pseudomonas putida*, a gram-negative, aerobic, mobile rod which is

ubiquitously distributed in soils and surface waters, was selected as a test species in the present study. The aim of the study was to describe the toxicity of a set of diverse AgNPs to this organism in order to contribute to the environmental hazard assessment of AgNPs. AgNPs with different sizes and coatings were tested in order to analyze whether those characteristics are determinants of nanoparticle toxicity. Silver nitrate was tested for comparison. Results highlight *Pseudomonas* as a particularly sensitive species. A second aim of the study was therefore to compare the observed toxicity values with environmental silver concentrations, in order to provide an overview whether, and to what extent, current silver concentrations might pose a risk to environmental bacteria.

The growth inhibition assay with *Pseudomonas putida* was used which is standardized according to ISO 10712 (1995). This test is commonly used for hazard assessments of other pollutants such as pharmaceuticals in the environment (Zoumkova et al. 2007) or metals (Teodorovic et al. 2009). However, despite its widespread use and the general high sensitivity of bacteria to the various forms of silver, *Pseudomonas* has to our knowledge not been used previously for the hazard characterization of AgNPs.

## Experimental

All selected AgNPs are available from commercial sources, but were partly acquired through the FP7 project NanoFATE (nAg1 and nAg7) and the German R&D project UMSICHT (nAg2 and nAg3), see acknowledgements. An overview of suppliers, reported primary particle size (diameter), reported silver content and coating as well as the stabilizing agents in the solution is given in Table 1.

## Preparation of test dispersions

All particles were delivered in aqueous dispersions, except nAg7 (powder) and nAg3 (viscous liquid). Pre-dilutions were made in Milli-Q water, which was necessary for all tested particles due to their high toxicity. nAg7 and nAg3 were weighed and dispersed in Milli-Q water for preparing the stock dispersion. nAg7 was prepared according to the protocol given by the suppliers, i.e. 30 seconds sonication after mixing with Milli-Q water to separate micron sized agglomerates. The nAg3 dispersion contained a stabilizing agent (4% Polyoxyethylene Glycerol Trioleate and Polyoxyethylene (20) Sorbitan mono-Laurat (Tween 20), which was also tested for toxicity in its pure form (supplied by the manufacturer) without any nanoparticles present. The stabilizing agent did not cause any toxicity up to the concentration that is present in the nAg3 dispersion at 100% toxicity (data not shown).

Table 1. Properties of the tested silver nanoparticles according to the suppliers' information.

## Nanoparticle characterization

An initial range finding proved that both the silver nitrate as well as the silver nanoparticles caused strong toxic effects to *Pseudomonas putida*.

Neither particle behavior nor dissolved silver concentrations could be determined during the tests, as particle numbers and silver concentrations were too close to or even below the limit of detection and quantification for standard ICP-MS analyses, the NanoSight Nanoparticles Tracking Analysis (NTA) (level of detection approx.  $10^6$  particles/mL) and Transmission Electron Microscopy (TEM). Well dispersed individual nanoparticles can be imaged successfully in TEM with a concentration of 10 to 100 mg/L. However, if a large percentage of nanoparticles are in agglomerates, the necessary concentration may be as high as 1000 mg/L. Hence, stock dispersions were

analyzed prior to the experiments with TEM to ascertain information about the nanoparticle quality, shape and the homogeneity of the dispersion. Diluted stock dispersions in Milli-Q water, which formed the basis for the dilution series in the actual test medium, were checked for particle behavior and particle concentration with NTA.

### **Transmission Electron microscopy (TEM)**

Experiments were carried out on a JEOL 2010 analytical TEM (JEOL Ltd, Japan), equipped with a LaB<sub>6</sub> electron gun and operated between 80 and 200kV. Samples were dispersed in water and a drop of the dispersion was deposited on a holey carbon coated copper TEM grid and dried at room temperature for several hours before examination. Depending on the concentration of the stock dispersion between 10 and 149 particles were checked per sample, details on observed particle numbers and standard deviation are given in Table 3.

### **NanoSight Nanoparticle Tracking Analysis (NTA)**

Particle concentrations and size distributions of the stock dispersions were checked with NTA, using a LM10HSBF (NanoSight Ltd, Amesbury United Kingdom) equipped with a 405nm laser and an EMCCD camera. Each sample of the stock dispersion was measured in 3 independently taken samples from the stock dispersions. Table 2 gives the average values for these measurements for the particle number concentration as well as the determined average hydrodynamic diameter.

# **Growth inhibition assay with *Pseudomonas putida***

*Pseudomonas putida* (DSM 50026) was purchased freeze dried from the German Collection of Microorganisms and Cell Cultures (DSMZ) in Braunschweig, Germany. All components for preparing the bacterial culture and test media were purchased from Sigma-Aldrich (Stockholm, Sweden). The growth inhibition assay was performed according to ISO guideline 10712 (1995). For this purpose the initial bacteria culture was transferred into 200 mL sterilized culture medium (details of the culture medium composition are given in Table 2) in an Erlenmeyer flasks (closed by cotton wool) and placed on a magnetic stirrer.

Table 2: Overview on the composition of the culture medium and the test medium (pH 7) according to ISO guideline 10712 (1995).

Optical density was measured daily at 596 nm in a plate reader ( $\mu$ Quant<sup>TM</sup>BioTek Instruments, Inc.) by transferring a subsample of the bacterial culture to a 96 well plate (ultra low attachment, standard plate, VWR, Sweden). Blanks were measured to correct the optical density for medium turbidity. As soon as the culture reached an optical density of 0.2, which is indicative of the late exponential growth phase, it was diluted by a factor of 1000. This daily procedure ensured continuous exponential growth. Tests were carried out in 20 mL glass scintillation vials (Wheaton, VWR 218-2245, Sweden) using test medium (details on the medium composition are given in Table 2) with a test incubation time of 16 hours on a shaking unit with a shaking speed of 150 rpm. The difference between the culture medium and the test medium is the lack of yeast in the test medium. Stock cultures as well as tests were performed at 22 C +/-1°C.

Samples were transferred to a 96 well plate (low attachment, standard plate, VWR, Sweden) after the test and their optical density was measured at 700 nm as outlined above. Both media – culture and test medium – were prepared fresh every day from sterile filtered stock solutions using sterilized (autoclaved) Milli-Q water. According to the standard (ISO 10712) the stock solutions were stored in the refrigerator at 2° C to 4° C for a maximum of three weeks.

# **Determination of concentration-response curves**

For all particles and for silver nitrate full concentration-response curves were determined (0-100% effect) in at least two independent experiments. Each experiment covered the concentration range with 8 different concentrations in 3 replicates and a minimum of 6 untreated controls.

Results were pooled for the final determination of the concentration response relationships. These were modeled following the strategy described in Scholze et al. (2001), and a series of 12 different models were fitted to each data set. The best-fitting model was selected on the basis of the absolute errors and from a visual inspection of the residuals.

Frequently the effects at high concentrations were higher than 100%, i.e. the optical density after the exposure was below the optical density at the beginning of the experiment. This indicates that the cells underwent lysis. In order to account for this, the concentration-response models  $f(x)$  – which are initially confined to the range of 0% to 100% effect – were extended as follows:

$$f(x)_{modified} = \theta_{min} + (\theta_{max} - \theta_{min}) \times f(conc)$$

Details on the finally selected models and the corresponding parameter estimates are provided in the supporting information, table 1.

Effect concentrations ( $EC_{05}$ ,  $EC_{10}$  and  $EC_{50}$ ) were derived from the corresponding inverses of these function and the 95% confidence intervals (CI) were estimated using the standard Wald-based approach of SAS (Vers. 9.2, SAS Institute, Cary, USA). All concentration-response calculations were based on the TEM-determined size distribution and the NTA-determined particle numbers, assuming a spherical shape of the particles.

233

## 234 **Results**

235 Nanoparticle characterisation by Transmission Electron microscopy (TEM)

236 The TEM micrographs of all tested particles are shown in Figure 1.

237

238 Figure 1. TEM micrographs of the different silver nanoparticle dispersions. TEM micrographs were taken for an initial quality check of the purchased dispersions (or in case of the nAg7 (g)) the freshly dispersed powder in Milli-Q water) to get information on shape and homogeneity of the particles. Please be aware that the panels have different scale bars.

242 a) nAg1, 3-8 nm, no coating b) nAg2, 10 nm, no coating c) nAg3, 20 nm, no coating d) nAg4, 20 nm, citrate coated e) nAg5, 20 nm, tannic acid coated f) nAg6, 40 nm, citrate coated g) nAg7, 50 nm, powder, dispersed in Milli-Q water

245

246 The TEM micrographs generally revealed well defined homogenous spherical particles within the anticipated size range (Figure 1 a-g), with the exception of the nAg7 particles (Figure 1g) which show rather heterogeneous shapes and a broad size distribution. The nAg2 dispersion (Figure 1 b) consisted of spherical particles but with a broad size range distribution of the primary particles (10 – 50 nm). The TEM picture of the nAg5 nanoparticles unexpectedly showed a dark inner core which was identified as a gold core by Energy dispersive X-ray spectroscopy (TEM-EDX).

The effect concentrations listed in Table 4 are based on total silver and the assumption that the particles consist of silver only and are spherical. Therefore the nominal effect concentrations presented for nAg5 are an underestimation, as the amount silver dissolving from the particles and the resulting actual silver concentration in the test medium is lower than calculated.

The listed effect concentrations are likely only a rough estimate in case of the nAg7 particles, because of their pronounced dispersion heterogeneity.

### **Nanoparticle Tracking Analysis (NTA)**

Particle concentrations and average particle sizes of the Milli-Q stock dispersions obtained with Nanoparticle Tracking Analysis (NanoSight) are presented in Table 3.

The average size of the Ted Pella, Inc. (nAg4, nAg5), British Biocell International (nAg6) and nAg3 particles were in accordance with supplier provided information. nAg2 particles, however, had an actual (NTA-determined, data not shown) size of 53 nm instead of the nominal 10 nm, corresponding to the heterogeneous size distribution of 10 to 50 nm that was observed for the primary particles in the TEM (Figure1 b, Table 3).

Also the nAg1 particles were bigger than anticipated (NTA determined 63 nm instead of 3-8nm, NTA data not shown) in average, which can be attributed to loose agglomerates of the 3-8nm primary particles (Figure 1 a).

Tab. 3. Size and particle concentration of the diluted AgNP stock dispersions (in Milli-Q) as determined from TEM and NanoSight Nanoparticle Tracking Analysis (NTA).

## 278 Toxicity to *Pseudomonas putida*

279 Exposure to AgNO<sub>3</sub> as well as AgNPs caused high toxicity to *Pseudomonas*. In some  
280 cases growth inhibitions higher than 100 % were observed, indicating cell lysis.  
281 Reliable concentration-response relationships could be determined for all particles,  
282 with EC<sub>05</sub>, EC<sub>10</sub> and EC<sub>50</sub> values in the low µg L<sup>-1</sup> range (Table 4).

283

284 Tab. 4: Overview of EC<sub>05</sub>, EC<sub>10</sub> and EC<sub>50</sub> values in µg L<sup>-1</sup> total silver. Details on parameter estimates  
285 and concentration-response models are given in the supporting information, Table 1 and overview on  
286 the curve fits to the raw data is given in Figure 2.

287 \*values in brackets denote approximate 95% confidence intervals

288

289 AgNO<sub>3</sub> is the most toxic agent tested (EC<sub>10</sub> = 0.058 µg L<sup>-1</sup>), although the toxicity of  
290 nAg3 and nAg5 also reaches very low levels (nAg3, EC<sub>10</sub> = 0.15µg L<sup>-1</sup>, and nAg5,  
291 EC<sub>10</sub> = 0.34 µg L<sup>-1</sup>). The other particles were less toxic, with 10 to 85 times higher  
292 EC<sub>10</sub> values (Table 4). Specifically for nAg5 the true EC values, based on total silver,  
293 might be lower than provided, because TEM-EDX proved that this specific particle  
294 possessed a gold core, which implies a lower total amount of silver dissolved from of  
295 the particles.

296 Figure 2 presents the fits to the inhibition data for all tested compounds in the growth  
297 inhibition assay with *Pseudomonas putida*.

298

299 Figure 2. a) – g) gives an overview on the inhibition data and the curve fits for all tested compounds,  
300 stating the respective used model as well as the number of performed independent experiments.

301

302 Figure 2 also visualizes the different slopes of the concentration response curves of  
303 the different particles. The ratio of EC<sub>50</sub> to EC<sub>05</sub>, which can serve as a measure for the  
304 steepness of the concentration response curve in the lower effect-range, ranges from x

for nAg3 to y for nAg7 indicating different dissolution kinetics and/or modes of toxic action.

The lowest EC<sub>50</sub> value, was observed for the nAg3 particles with 0.25 µg L<sup>-1</sup>, the highest EC<sub>50</sub> value was determined for nAg4 particles (13.4 µg L<sup>-1</sup>). The citrate coated 40 nm particles (nAg6) have an EC<sub>50</sub> of 2.4 µg L<sup>-1</sup> and are hence more than a factor of five more toxic than the smaller 20 nm particles (nAg4, EC<sub>50</sub> 13.4 µg L<sup>-1</sup>), whereas the tannic acid coated AgNPs (nAg5) show roughly the same toxicity (EC<sub>05</sub> 0.22 µg L<sup>-1</sup>) than the uncoated 20 nm AgNPs (nAg EC<sub>05</sub> 0.13 µg L<sup>-1</sup>) on an EC<sub>05</sub> level, but the uncoated 20 nm particles (nAg3, EC<sub>50</sub> 0.25 µg L<sup>-1</sup>) are approximately a factor of 4 more toxic than the 20 nm tannic acid coated particles (EC<sub>50</sub> 1.03 µg L<sup>-1</sup>) on an EC<sub>50</sub> level.

## Discussion

Silver is known to be highly toxic to aquatic wildlife. In fact, the metal is second only to mercury in its toxicity (Fries et al. 2010) and its toxicity has been described in a broad range of studies with vertebrates and invertebrates alike ( Fabrega et al, 2011). Prokaryotic organisms such as *Escherichia coli*, nitrifying bacteria, *Pseudomonas fluorescence* or *Pseudomonas putida* biofilms tend to belong to the more sensitive organism groups, EC<sub>50</sub> values are typically in the µg Ag L<sup>-1</sup> range (Fabrega et al. 2009; Fabrega et al. 2011). The bulk of EC<sub>50</sub> values for *Escherichia coli* falls into the range of 1 to 10 mg L<sup>-1</sup> (Hwang et al. 2008; Lok et al. 2006; Morones et al. 2005), Comparing these data to the EC<sub>50</sub> values presented in table 4 (0.25-13.4 µg L<sup>-1</sup>) shows that *Pseudomonas putida* is more sensitive than *Escherichia coli* in average. However, Pal and coworkers (2007) recorded lower EC<sub>50</sub> values for *Escherichia coli* (0.1-10 µg L<sup>-1</sup>), and Lok et al (2006) even reported EC<sub>50</sub> values between 43 - 86 ng

L-1 matching the here presented results much better than the average values between 1 and 10 mg L<sup>-1</sup>. The precise reasons behind these enormous differences in the reported *Escherichia coli* EC<sub>50</sub> values are currently unknown. It should be noted, however, that in general the test conditions are very different with differing temperatures as well as different test media being the two main drivers for varying silver bioavailability. The lower EC<sub>50</sub> values reported Lok et al (2006) were recorded at 37°C, i.e. at 15 °C higher temperature than it was used in the present study. The correspondingly increased dissolution of the silver particles might therefore explain the higher toxicity at higher temperatures.

Toxicity to bacteria is also heavily influenced by the life style of the exposed bacteria, as demonstrated by Sheng and co-workers (2011) who comparatively analyzed the toxicity of AgNPs on bacterial biofilms and planktonic bacteria. They found only low toxicities when exposing biofilms (effects occurred only at concentrations > 200 mg L<sup>-1</sup> after 24 hours incubation time) but with a dramatic increase in toxicity when the bacteria were extracted from the biofilm and tested in their planktonic form. Under these conditions all bacteria died already after an exposure of 1 mg L<sup>-1</sup> over only one hour, a phenomenon that is most likely driven by an increased bioavailability. This corresponds well with the high sensitivity of the planktonically living *Pseudomonas*, as reported in the present study.

Radniecki and co-workers (2011) found 20 nm particles to be more toxic than 80 nm particles, which was attributed to the higher release rate of Ag<sup>+</sup> ions from the smaller particles with a bigger surface area per mass. This hypothesis was also in concordance with studies from Pal et al. (2007) and Sadeghi et al. (2012) who both investigated the influence of different nanoparticle shapes (rods, triangles, spherical particles) on

bacterial toxicity. Both conclude that certain shapes increase or decrease the toxicity of AgNPs which can be explained by an increased or decreased surface area of the particles releasing more or fewer  $\text{Ag}^+$  ions.

However, the assumption that the smallest primary particles were most toxic did not hold true in the present study, as the nAg1 particles with a TEM-determined diameter of 3-8 nm only had an intermediate toxicity ( $\text{EC}_{50}$  value =  $3.4 \mu\text{g L}^{-1}$ ), far lower than the 20nm particles nAg3 ( $\text{EC}_{50}$  value =  $0.25 \mu\text{g L}^{-1}$ ). The fact that the nAg1 particles were present in loosely bound agglomerates already in the stock suspension will most likely have led to a reduced  $\text{Ag}^+$  ion release into the medium (due to the lower volume to surface ratio) and therefore to a lower toxicity than expectable from the small primary particle size. The same holds true for the nAg2 particles. Using the NTA data, which sized nAg1 as well as nAg2 particles in the range  $>50\text{nm}$  diameter, i.e. similar to the nAg7 particles, correlates better with the observed toxicity ranking. (nAg3  $>$  nAg7  $\sim$  nAg1  $\sim$  nAg2). However, NTA is limited to silver particles with a diameter of 20nm or higher and analytical samples have to have a relatively high particle concentration. NTA is therefore not directly suitable for the monitoring of environmentally relevant concentrations which are typically in the low  $\mu\text{g/L}$  range. (Carr and Wright, 2013).

Tannic acid and citrate are both loosely attached coatings (citrate more than tannic acid, nanoComposix, December 2013). Citrate can easily be displaced with other molecules (e.g. proteins or other compounds from the growth medium) for binding studies or custom functionalization; tannic acid can be replaced by molecules with strongly binding functional groups. Both, citrate and tannic acid provide a high degree

of electrostatic stabilization and therefore contribute to the colloidal stability of the particles, preventing them from agglomeration and therefore increasing their dissolution rate. Results from Ahmed et al. (2010) investigated the influence of the coating on AgNP toxicity and found that coated AgNPs caused more severe DNA damage than uncoated particles, caused by the lower surface area of the uncoated particles as a result of their agglomeration. A similar result was also found by Aranout and co-workers (2012) who investigated the effects of three different coatings (citric acid, gum arabicum (GA) and polyvinylpyrrolidone (PVP)) coated AgNPs and found that the citrate and the GA clearly increased the toxicity towards *Nitrosomonas europaea*, most likely due to a higher  $\text{Ag}^+$  ion release rate.

However, the findings of the present study point to a more complex interaction between coating and toxicity to *Pseudomonas*: while the most toxic particles (nAg3) were uncoated, citrate coated particles of the same diameter (nAg4) were less toxic but tannic acid coated particles (nAg5) were, again, more toxic, despite the fact that those particles contain a gold-core and hence the total silver based effect concentrations in Table 3 are an underestimation for nAg5. So far it is unclear whether the observed high toxicity of the nAg5 particles is, at least partly, caused by particle-specific effects of the insoluble gold core.

There seems to be a general agreement in the literature that the resulting concentration of silver ions is the most important driver for the toxicity of silver nanoparticles, which is confirmed by the results obtained in this study as the determined ECx values for silver nitrate were approximately one order of magnitude lower than for the tested nanoparticles. Xiu and coworkers (2012) recorded the toxicity of AgNPs to

405 *Escherichia coli* under strictly anaerobic conditions in order to avoid Ag oxidation  
406 and inferred that “Ag<sup>+</sup> is the definitive molecular toxicant”, in particular because the  
407 toxicity of various differently sized, shaped and coated particles strictly followed the  
408 concentration-response pattern observed for AgNO<sub>3</sub> (Xiu et al 2012). Similar  
409 conclusions were drawn by Radniecki and coworkers (2011).

410 However, there is still an ongoing discussion in the literature on whether and to what  
411 extent particle specific effects contribute to the overall toxicity. The comparably high  
412 toxicity of the gold core particles with the silver shell (nAg5) seems to indicate a  
413 particle specific toxicity contribution, because the total silver based effect  
414 concentration in Table 3 is an underestimation for nAg5. Such particle specific effects  
415 were also found by Morones and co-workers (2005), who demonstrated that selected  
416 gram-negative bacteria (e.g. *Escherichia coli*, *Vibrio cholera*, *Pseudomonas*  
417 *aeruginosa*) react with the formation of so-called low molecular weight regions (a  
418 defense mechanism to protect the DNA) when exposed to silver nitrate, but not to  
419 AgNPs. Also Ortega-Calvo and co-workers (2011) found particle related effects on  
420 the tactic motility of *Pseudomonas putida*: the bacteria were repelled by AgNPs but  
421 not by AgNO<sub>3</sub>, suggesting a particle specific effect. The results presented in this study  
422 (Table 4, Figure 3) show that ionic silver is the most toxic silver form; the toxic  
423 effects of the different particles are lower. However, different amounts of total silver  
424 are needed for causing a certain effect of the different particles (Table 4, Figure 3),  
425 which indicates that the observed toxicity is not caused simply by ionic silver from  
426 dissolved particles. However, the precise role and interaction of possibly different  
427 dissolution, aggregation and uptake kinetics and particle-specific effects remains a  
428 subject for further studies, as soon as sufficiently sensitive analytical techniques are  
429 available.

Figure 3: Graphical overview of the recorded EC<sub>05</sub> values for AgNO<sub>3</sub> and the seven tested AgNPs in this study in relation to the silver concentrations found in surface waters of various geographical regions (numerical data and references for the surface water concentrations of the silver are given in the supporting information).

### **Risks of silver for environmental bacteria**

The recorded toxicity data, with EC<sub>05</sub> values between 0.043 µg L<sup>-1</sup> and 3.41 µg L<sup>-1</sup> highlight *Pseudomonas putida* as a particularly sensitive species. In order to analyse whether current environmental concentrations of silver approach toxic levels, silver concentrations from environmental monitoring studies of surface waters from various regions were compared to the recorded toxicity values (Figure 3, all numerical data and references are provided in the supporting information). The EC<sub>05</sub> value for AgNO<sub>3</sub> (0.043 µg L<sup>-1</sup>) recorded in this study is clearly below some of the silver concentrations monitored in German rivers with mean values between 0.06 and 0.7 µg L<sup>-1</sup> (Hund-Rinke et al. (2008)). Here, concentrations of up to 65 µg L<sup>-1</sup> silver were detected in Bavaria in 2006 (mean=1.17 µg L<sup>-1</sup>, the average concentrations in various German counties in 2000-2007 fall between 0.05 – 1.17 µg L<sup>-1</sup>). Ahmed and coworkers (2012) also determined silver concentrations in the µg L<sup>-1</sup> range in a heavily industrialized area in Bangladesh (max=14.9 µg L<sup>-1</sup>, mean=5.23 µg L<sup>-1</sup>). However, most other analytical surveys reported concentrations in surface water are in the ng L<sup>-1</sup> range (see Figure 3). Roditi et al. (2000) even determined dissolved silver concentrations below 0.1 ng L<sup>-1</sup> for lake Erie, Ontario and the Niagara and Hudson rivers, corresponding to total (unfiltered) concentrations between 1.3 and 8.3 ng L<sup>-1</sup>. It should be pointed out that the analytical survey was conducted already in 1997 and it is not known whether the continuously increasing use of silver and silver nanoparticle containing products has led to increased silver concentrations in those river systems since then.

This extremely broad range of environmental silver concentrations, which span six orders of magnitude, indicates that a general conclusion on whether the current use of silver and silver nanoparticles constitutes an environmental risk cannot be drawn. A case-by-case evaluation is needed instead. The EC<sub>05</sub> values that were recorded in the present study for the different particles differ only by a factor of less than 100, small in comparison to the dynamics in environmental concentrations. However, a good proportion of analytical determined silver concentrations are in a range that directly affects the growth pattern of *Pseudomonas putida* (Figure 3), a common environmental bacterium.

## Conclusions

The primary objective of this study was to contrast the effects of different silver nanoparticle sizes (with the following diameters of the primary particles: 3-8 nm, 10 nm, 20 nm, 40 nm and 50 nm) as well as different coatings (uncoated, citrate coated and tannic acid coated) with the toxicity of ionic silver (silver nitrate) to the gram-negative bacterium *Pseudomonas putida*.

The results showed no simple clear-cut relation between the toxicity of the different particles and their shapes and coatings. Assuming that the final toxic effect of a given AgNP is driven by its ion-release kinetics, it can be assumed to be linked to its coating (preventing agglomeration), the primary particle size (higher release rate from smaller particles), the agglomeration status, the medium components and the exposure conditions (e.g. light, oxygen concentrations) (Fabrega et al. 2011; Marambio-Jones and von Hoek 2010). However, the results indicate a more intricate interplay between these particle characteristics and the complex medium in which the tests needed to be carried out. The determination of the overall agglomeration behavior and ion release

482 kinetics remains highly challenging for test organisms as sensitive as *Pseudomonas*  
483 *putida*. Detection limits of the available characterization equipment, in particular in  
484 complex growth media, prevent a real time analysis of the exposure situation and  
485 definite conclusions on the particle behavior.

486

487 As the free ions generally represent the most toxic silver form, an environmental  
488 hazard assessment for aquatic microorganisms that is based on the total silver content  
489 should be sufficiently protective. However, the hazard profiles of free silver and silver  
490 nanoparticles might differ substantially for higher organisms which might take up  
491 particles directly e.g. fish via their gills, which would then deliver silver ions directly  
492 to certain tissues. Available data seem to indicate that microorganisms are generally  
493 the most sensitive organism group, i.e. they would be driving the hazard assessment.  
494 In this context more data on the toxicity of silver and silver nanoparticles to algae,  
495 one of the cornerstones of the standard “base set” of ecotoxicological data, used e.g.  
496 within REACH or the Biocide Regulation (EU) 528/2012, would improve the current  
497 understanding of the environmental risks of silver and silver nanoparticles.

498

#### 499 **Acknowledgements**

500 The authors thank the following people for their support and helpful discussions:

501 Åsa Arrhenius (University of Gothenburg) for support with the experiments, Mark  
502 Ware (NanoSight) for help with recording the NTA videos, Jurgen Arning and Juliane  
503 Filser (University of Bremen) for supplying the NM-300K and PL-Ag-S10 particles  
504 in the context of the UMSICHT R&D project (Federal Ministry of Education and  
505 Research, Germany, 03X0091).

506

507 **Funding sources and conflict of interest**

508 The study was financially supported by the Swedish Research Council (projects  
509 NanoRisk and NanoSphere) and the European Commission (FP7 project NanoFATE,  
510 NMP4-SL-2010-24773). The authors declare that they have no conflict of interest.

511 Supplementary data associated with this article can be found in the online version of  
512 this article in the supporting information.

513

514 **References**

515 Ahamed M, Posgai R, Gorey TJ, Nielsen M, Hussain SM, Rowe JJ (2010) Silver  
516 nanoparticles induced heat shock protein 70, oxidative stress and apoptosis in  
517 *Drosophila melanogaster*. *Toxicol Appl Pharmacol* 242: 264–269.

518

519 Ahmed G, Miah MA, Anawar HM, Chowdhury DA, Ahmad JU (2012) Influence of  
520 multi-industrial activities on trace metal contamination: An approach towards surface  
521 water body in the vicinity of Dhaka Export Processing Zone (DEPZ). *Environ Monit*  
522 *Assess* 184 (7): 4181-4190.

523

524 Aranout CL, Gunsch CK (2012) Impacts of Silver Nanoparticle Coating on the  
525 Nitrification Potential of *Nitrosomonas europaea*. *Environ Sci Technol* 46 (10):  
526 5387-5395.

527

528 D’Britto V, Kapse H, Babrekar H, Pabhune AA, Bhoraskar SV, Premnath V, Prasad  
529 BLV (2011) Silver nanoparticle studded porous polyethylene scaffolds: bacteria  
530 struggle to grow on them while mammalian cells thrive. *Nanoscale* 3 (7): 2957-2963.

531 Carr B, Wright (2013) Nanoparticle Tracking Analysis – a review of applications and  
532 usage 2010-2012. *NanoSight*.

533

534 Fabrega J, Renshaw JC, Ead JR (2009) Interactions of Silver Nanoparticles with  
535 *Pseudomonas putida* Biofilms. *Environ Sci Technol* 43: 9004–9009.

536

537 Fabrega J, Luoma SN, Tyler CR, Galloway TS, Lead JR (2011) Silver nanoparticles:  
538 Behaviour and effects in the aquatic environment. *Environ Internat* 37: 517-531.

539

540 Feng Q, Wu J, Chen G, Cui F, Kim T, Kim J (2000) A mechanistic study of the  
541 antibacterial effect of silver ions on *Escherichia coli* and *Staphylococcus aureus*. *J*  
542 *Biomed Mater Res* 52: 662-668.

543

544 Fries R, Gressler S, Simko M, Gazso A, Fiedeler U, Nentwich M (2010) Nanosilver.  
545 Nanotrust Dossiers No. 10.

546

547 Gottschalk F, Sonderer T, Scholz RW, Nowack B (2010) Possibilities and limitations  
548 of modelling environmental exposure to engineered nanomaterials by probabilistic  
549 material flow analysis. *Environ Toxicol Chem* 29 (5): 1036-1048.

550

551 Gottschalk F, Sonderer T, Scholz RW, Nowack B (2009) Modelled Environmental  
552 Concentrations of Engineered Nanomaterials (TiO<sub>2</sub>, ZnO, Ag, CNT, Fullerenes) for  
553 Different Regions. *Environ Sci Technol* 43 (24): 9216-9222.

554

555 Griffitt RJ, Luo J, Gao J, Bonzongo JC, Barber DS (2008). Effects of particle  
556 composition and species on toxicity of metallic nanomaterials in aquatic organisms.  
557 *Environ Toxicol Chem* 27: 1972–1978.

558

559 Griffitt RJ, Hyndman K, Denslow ND, Barber DS (2009) Comparison of molecular  
560 and histological changes in zebrafish gills exposed to metallic nanoparticles. *Toxicol*  
561 *Sci* 107 (2): 404-415.

562 <http://www.nanocomposix.com>, December 2013; nanoComposix Inc. 4878 Ronson  
563 Court, Suite K, San Diego, CA 92111, USA

564

565 <http://www.nanotechproject.org>, June 2012

566

567 Hund-Rinke KC, Schlich A, Wenzel A (2011) TiO<sub>2</sub> nanoparticles - relationship

568 between dispersion preparation method and ecotoxicity in the algal growth test.

569 Umweltwiss Schadst Forsch 22: 517-528.

570

571 Hwang ET, Lee JH, Chae YJ, Kim YS, Kim BC, Sang BI (2008) Analysis of the toxic

572 mode of action of silver nanoparticles using stress-specific bioluminescent bacteria.

573 Small 4: 746-750.

574

575 ISO Guideline 10712. 1995. Water quality – *Pseudomonas putida* growth inhibition

576 test.

577

578 Li M, Zhu L, Lin D (2011) Toxicity of ZnO Nanoparticles to *Escherichia coli*:

579 Mechanism and the influence of medium components. Environ Sci Tech 45 (5): 1977-

580 1983

581 Lok C, Ho C, Chen R, He Q, Yu W, Sun H (2006) Proteomic analysis of the mode of

582 antibacterial action of silver nanoparticles. J Proteome Res 5: 916-924.

583

584 Marambio-Jones C, Van Hoek EMV (2010) A review of the antibacterial effects of

585 silver nanomaterials and potential implications for human health and the environment.

586 J Nanopart Res 12: 1531–1551.

587

588 Miao AJ, Schwehr KA, Xu C, Zhang SJ, Luo Z, Quigg A (2009) The algal toxicity of

589 silver engineered nanoparticles and detoxification by exopolymeric substances.

590 Environ Pollut 157: 3034-3041.

591

592 Mitrano DM, Leshner EK, Bednar A, Monserud J, Higgins CP, Ranville JF (2012)  
 593 Detecting nanoparticulate silver using single-particle inductively coupled plasma-  
 594 mass spectrometry. *Environ Toxicol Chem* 31(1): 115-121.  
 595  
 596 Morones JR, Elechiguerra JL, Camacho A, Holt K, Kouri JB, Ramirez JT, Yacaman  
 597 MJ (2005) The bactericidal effect of silver nanoparticles. *Nanotechnology* 16 (10):  
 598 2346–2353.  
 599  
 600 Mueller NC, Nowack B (2008) Environmental Impacts of Nanosilver. *Environ Sci*  
 601 *Tech* 42: 4447-4453.  
 602  
 603 Navarro E, Piccapietra F, Wagner B, Marconi F, Kaegi R, Odzak N, Sigg L, Behra R  
 604 (2008) Toxicity of Silver Nanoparticles to *Chlamydomonas reinhardtii*. *Environ Sci*  
 605 *Technol* 42: 8959–8964.  
 606  
 607 Nowack B (2010) Nanosilver Revisited Downstream. *Science* 330: 1054-1055.  
 608  
 609 Nowack B, Krug H and Height M (2011) 120 years of Nanosilver history:  
 610 Implications for policy makers. *Environ Sci Technol* 45 (4): 1177 – 1183.  
 611  
 612 Ortega-Calvo JJ, Molina R, Jimenez-Sanchez C, Dobson PJ, Thompson IP (2011)  
 613 Bacterial tactic responses to silver nanoparticles. *Environ Microb Reports* 3 (5): 526-  
 614 534.  
 615  
 616 Pal S, Tak KY and Song JM (2007) Does the Antibacterial Activity of Silver  
 617 Nanoparticles Depend on the Shape of the Nanoparticle? A Study of the Gram-  
 618 Negative Bacterium *Escherichia coli*. *Appl Environ Microb*: 1712-1720.  
 619

- 620 Radniecki TS, Stankus DP, Neigh A, Nason JA, Semprini L (2011) Influence of  
621 liberated silver from silver nanoparticles on nitrification inhibition of *Nitrosomonas*  
622 *europaea*. *Chemosphere* 85 (1): 43-49.  
623
- 624 Roditi HA, Fisher NS, Sañudo-Wilhelmy SA (2000) Field testing a metal  
625 bioaccumulation model for zebra mussels. *Environ Sci Technol* 34 (13): 2817-2825.  
626
- 627 Sadeghi B, Garmaroudi FS, Hashemi M, Nezhad HR, Nasrollahi A, Ardalan S,  
628 Ardalan S (2012) Comparison of the anti-bacterial activity on the nanosilver shapes:  
629 Nanoparticles, nanorods and nanoplates. *Adv Powder Technol* 23 (1): 22-29.  
630
- 631 Scholze M, Boedeker W, Faust M, Backhaus T, Altenburger R, Grimme LH (2001) A  
632 general best fit method for concentration-response curves and the estimation of low-  
633 effect concentrations. *Environ Toxicol Chem* 20: 448-457.  
634
- 635 Sheng Z, Yang L (2011) Effects of silver nanoparticles on waste water biofilms. *Water*  
636 *Research* 45: 6039-6050.  
637
- 638
- 639 Teodorovic I, Planojevic I, Knezevic P, Radak S, Nemet I (2009) Sensitivity of  
640 bacterial vs. acute *Daphnia magna* toxicity tests to metals. *Centr Eur J Biol* 4 (4):  
641 482-492.  
642
- 643 Xiu ZM, Zhang QB, Puppala HL, Colvin VL, Alvarez PJ (2012) Negligible particle-  
644 specific antibacterial activity of silver nanoparticles. *Nano Lett* 12 (8): 4271-4275.  
645
- 646 Yeo MK, Yoon JW (2009) Comparison of the effects of nano-silver antibacterial  
647 coatings and silver ions on zebrafish embryogenesis. *Mol Cell Toxicol* 5: 23-31.  
648

649 Zouňková R, Odráska P, Doležalová L, Hilscherová K, Marsálek B, Zouňkov B  
650 (2007) Ecotoxicity and genotoxicity assessment of cytostatic pharmaceuticals.  
651 Environ Toxicol Chem 26 (10): 2208-2214.

652  
653  
654  
655  
656  
657  
658  
659  
660  
661  
662  
663  
664  
665  
666  
667  
668  
669  
670  
671  
672  
673  
674  
675  
676  
677  
678

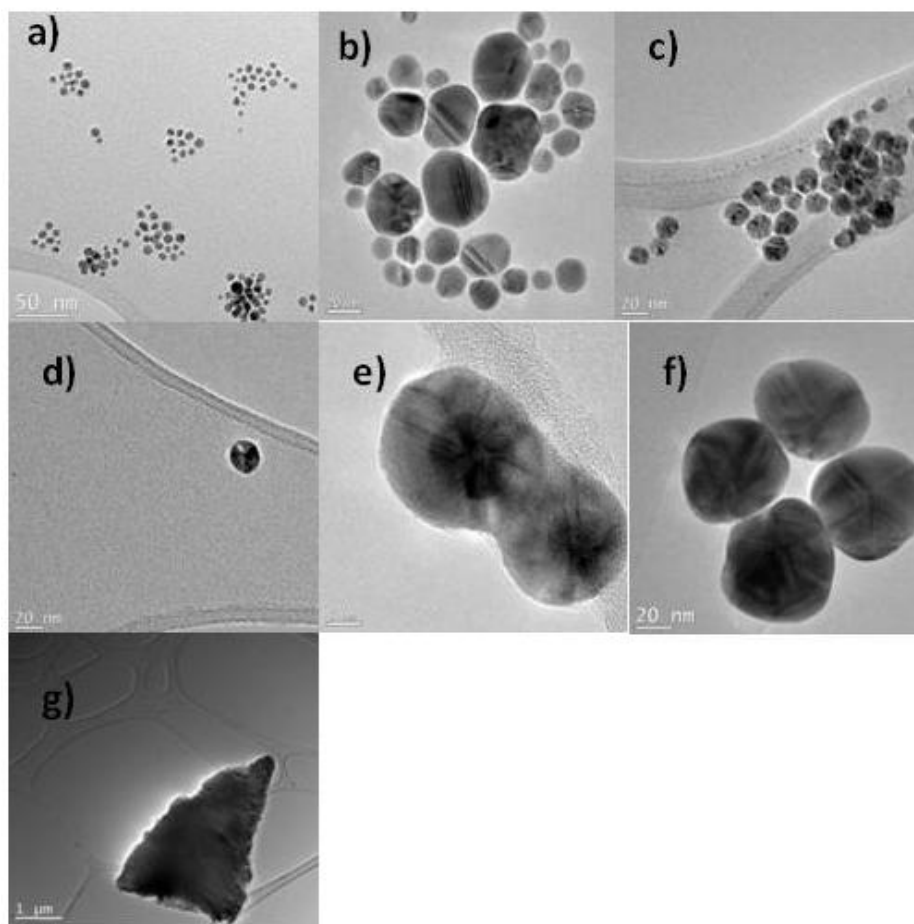
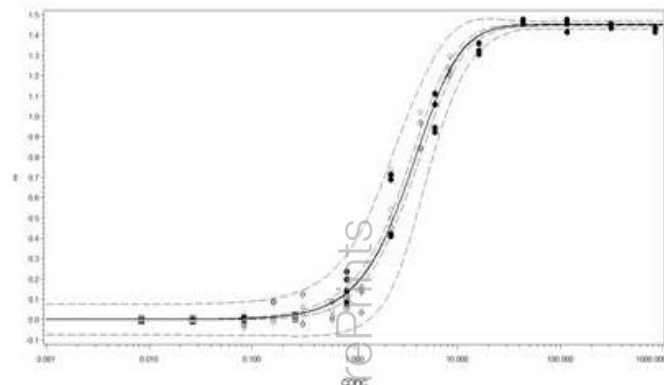
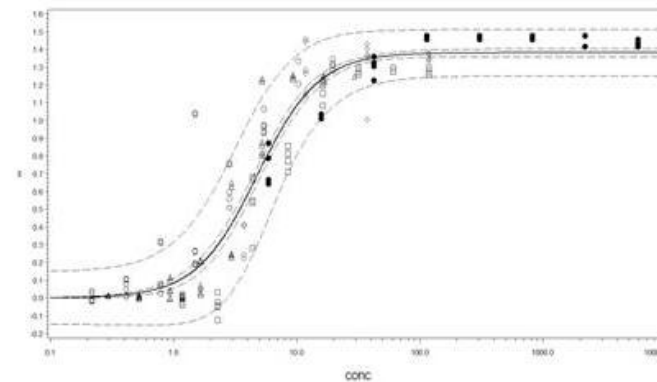


Figure 1. TEM micrographs of the different silver nanoparticle dispersions. TEM micrographs were taken for an initial quality check of the purchased dispersions (or in case of the nAg7 (g)) the freshly dispersed powder in Milli-Q water) to get information on shape and homogeneity of the particles. Please be aware that the panels have different scale bars.

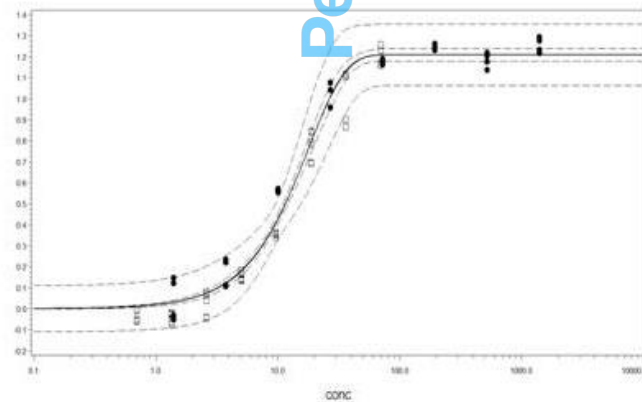
a) nAg1, 3-8 nm, no coating b) nAg2, 10 nm, no coating c) nAg3, 20 nm, no coating  
d) nAg4, 20 nm, citrate coated e) nAg5, 20 nm, tannic acid coated f) nAg6, 40 nm, citrate coated  
g) nAg7, 50 nm, powder, dispersed in Milli-Q water.



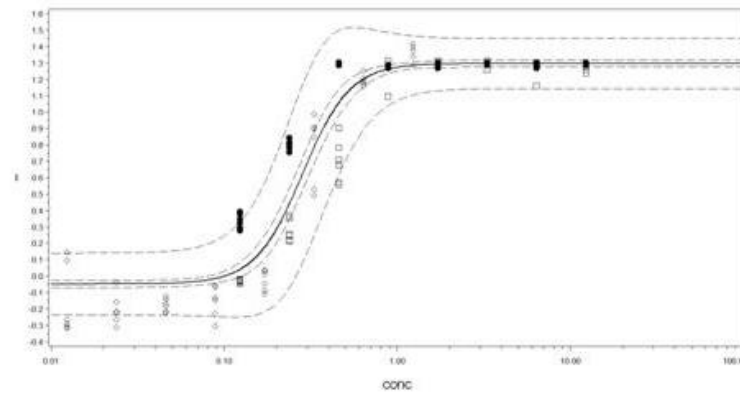
a) Curve fit (used model: Probit) to the raw data for silver nitrate, results from 3 independent experiments were pooled



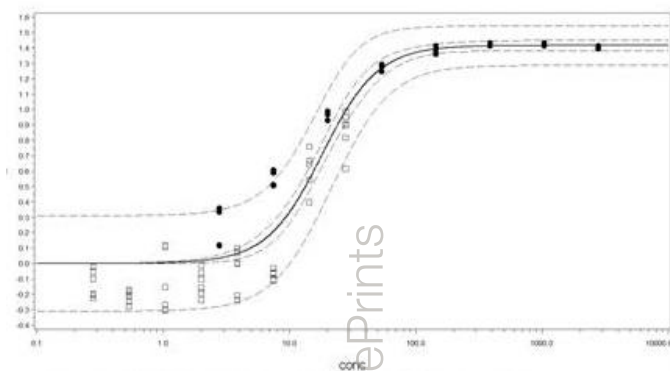
b) Curve fit (used model: Morgan-Mercer-Flodin) to the raw data for nAg1, results from 5 independent experiments were pooled



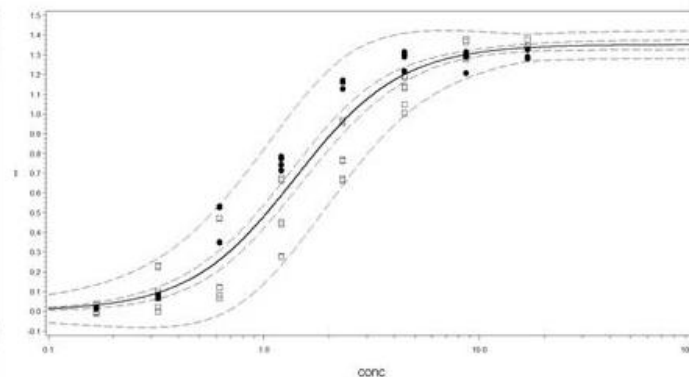
c) Curve fit (used model: Weibull) to the raw data for nAg2, results from 2 independent experiments were pooled



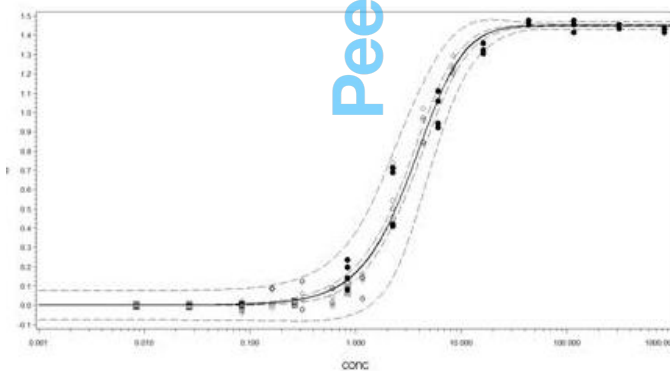
c) Curve fit (used model: Morgan-Mercer-Flodin) to the raw data for nAg3, results from 3 independent experiments were pooled



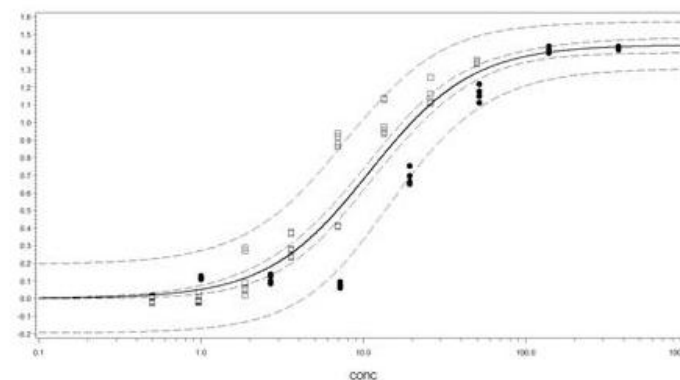
d) Curve fit (used model: Morgan-Mercer-Flodin) to the raw data for nAg4, results from 2 independent experiments were pooled



e) Curve fit (used model: Morgan-Mercer-Flodin) to the raw data for nAg5, results from 2 independent experiments were pooled



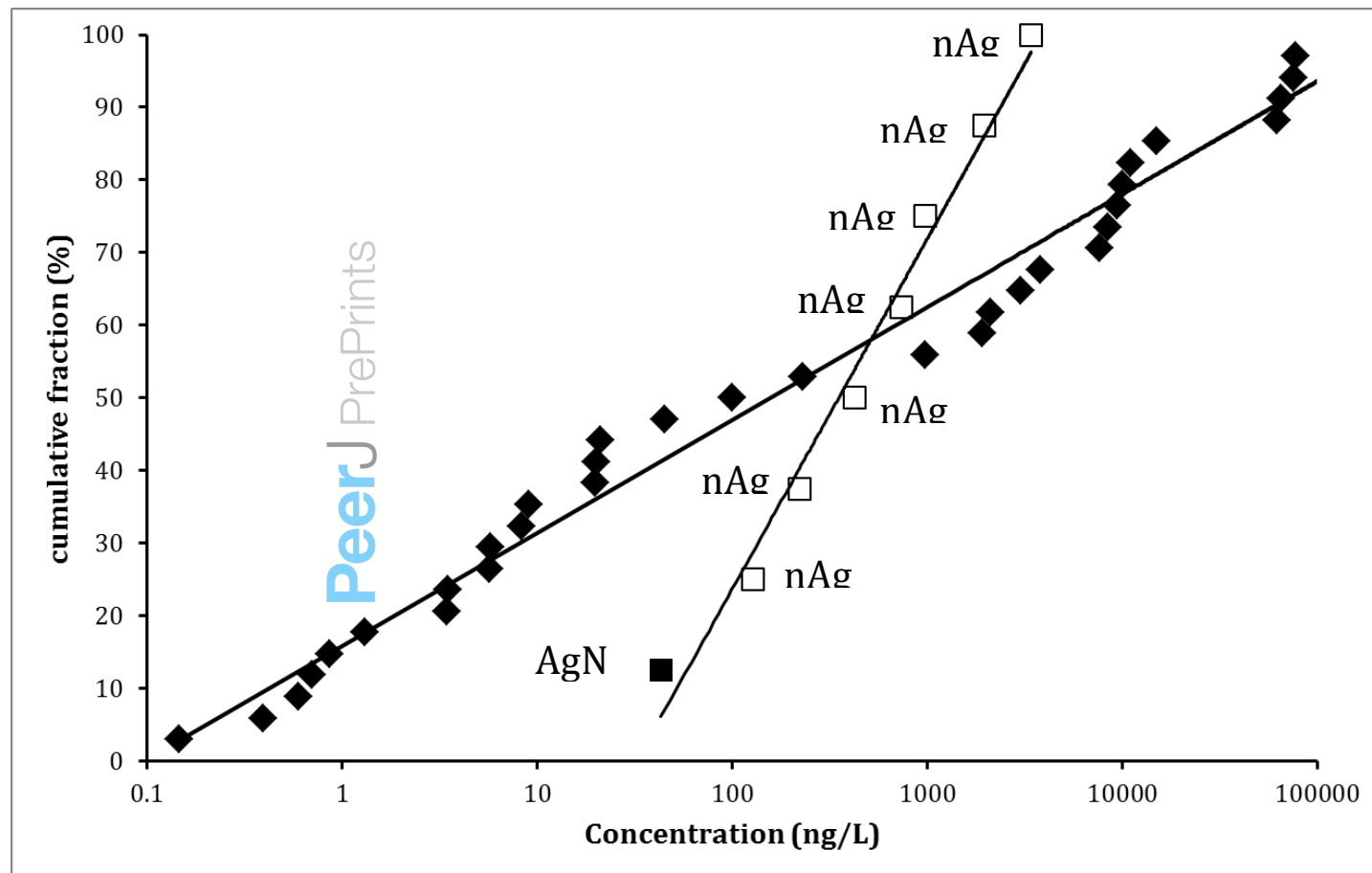
f) Curve fit (used model: Generalized Logit 2) to the raw data for nAg6, results from 3 independent experiments were pooled



g) Curve fit (used model: Morgan-Mercer-Flodin) to the raw data for nAg7, results from 2 independent experiments were pooled

690  
691  
692

Figure 2. a) – g) gives an overview on the raw data and the curve fits for all tested compounds, stating the respective models well as the number of performed independent experiments.



693

694

695

696

Figure 3. Graphical overview of the recorded  $EC_{05}$  values for  $AgNO_3$  and the seven tested AgNPs in this study in relation to the silver concentrations found in surface waters of various geographical regions (numerical data and references for the surface water concentrations of the silver are given in the supporting information).

697 Table1. Properties of the tested silver nanoparticles according to the suppliers' information.  
698

Acronym	Name	Supplier	Primary particle size, diameter (nm)	Coating	Particle concentration [particles/mL]	Silver concentration mg l-1	Medium	Stablising agent
AgNO <sub>3</sub>	AgNO <sub>3</sub>	Sigma Aldrich, Germany	-	-	-	-	Powder	
nAg1	AG7	Amepox, Poland	3-8	not specified	not specified	1000	Aqueous dispersion	not specified
nAg2	PL-Ag-S10	Plasmachem AG, Germany	10	not specified	not specified	100	Aqueous dispersion	not specified
nAg3	NM-300K	OECD WPMN program, JRC, Ispra, Italy	20	none	not specified	1000000	Aqueous dispersion	4% Polyoxyethylene Glycerol Trioleate and Polyoxyethylene (20) Sorbitan mono-Laurat (Tween 20)
nAg4	PELCO <sup>®</sup> NanoXact <sup>™</sup> (84060-20)	Ted Pella, Inc., USA	20	citrate	4.5*10 <sup>11</sup>	20	Aqueous dispersion	2 mM citrate buffered dispersion, pH 7.4
nAg5	PELCO <sup>®</sup> NanoXact <sup>™</sup> (84160-20)	Ted Pella, Inc., USA	20	tannic acid	4.5*10 <sup>11</sup>	20	Aqueous dispersion	2 mM citrate buffered dispersion, pH 7.4
nAg6	Silver colloid	British Biocell International, UK	40	citrate	9*10 <sup>9</sup>	n.d.	Aqueous dispersion	no preservatives, residual chemical left from manufacture (not specified)
nAg7	AG6	NanoTrade, Czech Republic	50	not specified	not specified	not specified	Powder	

699

700

701

702

703 Table 2. Overview on the composition of the culture medium and the test medium (both pH 7) according to ISO guideline 10712 (1995).

704

Nutrients	Culture medium mg L <sup>-1</sup>	Test Medium mg L <sup>-1</sup>
NaNO <sub>3</sub>	500	500
K <sub>2</sub> HPO <sub>4</sub> × 3H <sub>2</sub> O	120	120
KH <sub>2</sub> PO <sub>4</sub>	60	60
yeast extract	50	-
C <sub>6</sub> H <sub>12</sub> O <sub>6</sub>	2000	2000
MgSO <sub>4</sub> × 7H <sub>2</sub> O	200	200
iron(III) citrate	0.5	0.5

714

715

716

717

718

719

720

721

722

723

724

725

726

727

728

729

Table 3. Size and particle number concentration of the diluted silver nanoparticle stock dispersions (in Milli Q) as determined from Transmission Electron Microscopy (TEM) and NanoSight Nanoparticle Tracking Analysis (NTA).

Acronym	Average size, nm (TEM)	Number of observed particles (TEM)	Average size (hydrodynamic diameter) in nm (NTA)	Particle conc. [particles/mL] (NTA)*	silver conc. mg L <sup>-1</sup> based on NTA particle conc. and TEM size	nominal silver conc. mg L <sup>-1</sup>
nAg1	8 [+/-2]	61	63 [+/-28]	$2.1 \times 10^{14}$	590	1000
nAg2	14 [+/-8], but between 10 – 50 nm, mostly bound in loose aggregates	50	53 [+/-21]	$9.3 \times 10^{12}$	140	100
nAg3	20 [+/-3]	53	29 [+/-21]	$2.8 \times 10^{15}$	122505	100000
nAg4	20 [+/-4.5]	10	31 [+/-13]	$1.27 \times 10^{12}$	55	20
nAg5	20 [+/-3]	24	26 [+/-10]	$7.6 \times 10^{11}$	33	20
nAg6	40 [+/-7]	10	41 [+/-16]	$9 \times 10^9$ $7.6 \times 10^9$	2.6	3.16**
nAg7	60 [+/-11]: primary particles between 30 – 60 nm, bound in mirconsized agglomerates, possible to resuspend with sonification	149	85 [+/-29]	$3.9 \times 10^8$	0.46	0.1

\*NTA measurements are based on 3 independently taken samples

\*\*calculated based on the primary particle size and the particle number, no information about the silver content was given by the supplier

735

736 Table 4. Overview of EC<sub>05</sub>, EC<sub>10</sub> and EC<sub>50</sub> values in µg L<sup>-1</sup> total silver. Details on parameter estimates and concentration-response models are  
 737 given in the supporting information, Table 1 and an overview on the curve fits to the raw data is given in Figure 2.

738

Acronym	Particle size (TEM based)	Particle coating	EC <sub>05</sub>	EC <sub>10</sub>	EC <sub>50</sub>
AgNO <sub>3</sub>	none	none	0.043 [0.053-0.036]	0.058 [0.071-0.05]	0.16 [0.18-1.69]
nAg1	8 nm	none	0.73 [0.94-0.59]	1.11 [1.36-0.92]	3.46 [3.84-3.10]
nAg2	14 nm	none	1.96 [-]	3.24 [3.75-2.77]	11.6 [12.5-11]
nAg3	20 nm	none	0.13 [0.15-0.11]	0.15 [0.17-0.13]	0.25 [0.28-0.26]
nAg4	20 nm	citrate	3.41 [4.82-2.59]	4.93 [6.52-3.88]	13.4 [15.3-11.6]
nAg5	20 nm	tannic acid	0.22 [0.29-0.18]	0.34 [0.41-0.28]	1.03 [1.16-0.93]
nAg6	40 nm	citrate	0.42 [0.57-0.33]	0.69 [0.86-0.55]	2.40 [2.68-2.13]
nAg7	60 nm	none	0.98 [1.43-0.71]	1.66 [2.22-1.25]	6.9 [7.95-5.90]

739

740